JOURNAL OF THERMOPHYSICS AND HEAT TRANSFER
Vol. 23, No. 2, April–June 2009

Technical Notes

TECHNICAL NOTES are short manuscripts describing new developments or important results of a preliminary nature. These Notes should not exceed 2500 words (where a figure or table counts as 200 words). Following informal review by the Editors, they may be published within a few months of the date of receipt. Style requirements are the same as for regular contributions (see inside back cover).

Modeling of Heat Transfer in Cisterns Using Artificial Neural Networks

R. Madoliat*
Iran University of Science and Technology, 1684613114 Tehran, Iran
and
M. Razavi† and A.R. Dehghani‡
Islamic Azad University, 1418863753 Tehran, Iran

DOI: 10.2514/1.37043

Nomenclature

a	=	output of the transfer function
$a_j(k)$	=	Jth element of the artificial neural network's output related with input vector $P(k)$
a_q	=	network's output for p_q
a^0	=	input of the first layer
B	=	y intercept of the regression line in the scatter plot
b	=	bias
$e_j(k)$	=	Jth element of the error ways of
$F(k)$	=	summation of the error in the Kth frequency
f	=	transfer function of the layer
M	=	regression line slope in the scatter plot
perf	=	neural network's performance function (sum of squared error)
P_i	=	input vector of the network
R	=	correlation coefficient between the artificial neural network's output and observation
S^L	=	number of neurons in layer L
T_i	=	target vector for input P_i
$t_j(k)$	=	Jth element of the target vector related with input vector $P(k)$
ω	=	weight matrix of each layer

Subscript

J	=	Jth element of the answer network

Superscript

L	=	number of network layers

Received 7 February 2008; revision received 30 September 2008; accepted for publication 30 September 2008.

*Associate Professor, School of Mechanical Engineering; madoliat@iust.ac.ir.

†Graduate, Department of Mechanical Engineering, Science and Research Campus; masood_razavi60@yahoo.com.

‡Graduate, Department of Mechanical Engineering, Science and Research Campus; al_dehghani@hotmail.com.

Introduction

SAVING thermal energy is one of the most important ways of balancing accessible and required energy. It is also a promising method to decrease the consumption of fossil energy. Because of its importance, much effort has been devoted by industrialized nations to save thermal energy. For decades, water has been one of the most useful media for storage of thermal energy [1]. A comprehensive review of the studies on the concept of cold thermal energy storage (CTES) and its applications and on various kinds of CTES systems and their merits has been conducted by Saito [2].

Thermal stratification is frequently used in the thermal storage systems. Therefore, the main focus of the relevant studies has been on the influence of various design parameters on preserving the thermal stratification. Nelson et al. [3,4] investigated the effects of a storage tank's dimensions and its wall physical properties and the mixing effects of fluid flow during charging and discharging cycles on the decay of thermal stratification in a thermally stratified, vertical, cylindrical, chilled-water storage tank. Their results showed that increasing the length-to-diameter ratio of the tank prevents the degradation of thermal stratification; however, for aspect ratios greater than three, the effects were marginal. They also reported that the fluid flow during charging and discharging cycles degrades the existing thermal stratification inside the storage tank. The effect of the material of the storage tank on the development of thermal stratification during charging and discharging cycles was found to be insignificant; however, insulating the tank improved the thermal stratification.

Al-Marafie [5] experimentally analyzed the thermal stratification in a chilled-water storage tank, which was used for storing chilled water produced by an air-conditioning system during off-peak periods and delivering it throughout peak demand for the cooling load. He reported a tank extraction efficiency of nearly 90%. Suri et al. [6] conducted an experimental investigation on an air-conditioning system assisted by two cold-storage tanks. Their results showed that using a cool-storage-assisted system brought about a significant economic advantage by reducing the cooling cost by 25%. For the study of daily energy storage in tanks, researchers' main concerns are for evaluating thermal performance and developing thermal layering and its analysis in feeding-discharging periods of the system [7–12]. In comparison, not much research has been carried out in the long-term energy-saving systems. Bahadori and Haghighat [13] evaluated the thermal performance of a common water reservoir in a hot, arid region. In their research, the storage tank was assumed to be filled with cold water in the winter and to remain intact in the summer. The temperature distribution in water and soil around the reservoir was obtained by solving equations in various methods. Temperature distributions in various months of the year were obtained. It was observed that a thermal stratification formed in the storage tank. The temperature change in the upper layers was a function of temperature changes of the environment, whereas temperature changes in the bottom layers were low. Dehghan and Dehghani§ and Dehghan [14] experimentally studied the thermal layering of a long-term cold-water underground reservoir with a volume of 450 m^3; their results show that the thermal layering was stable during discharge periods. Lower layers of water with linear

§Private communication with A. Dehghan and A. R. Dehghani of Yazd University, 2002.

temperature distribution and upper layers of water with exponential temperature distribution were considered.

In this research, thermal layering in the long-term cold-water underground reservoir§ will be studied using artificial neural networks (ANNs). It should be noted that the study of neural networks commenced in the late 19th and early 20th centuries. Primary research summarized in [15] basically included theories in learning and special mathematical models of neurons. Modern views of neural networks started in 1943 with McCulloch and Pitts [16]. They proved that ANNs could be used to solve any kind of math or logical equation. Nowadays, their study is usually considered as a starting point for this field of research.

In recent years, the use neural networks for heat transfer studies has increased considerably [17–21]. Neural networks cannot generate a relation between two sets of numbers as a math function, but they can generate a transformation between an input–output series. This transformation gives acceptable outputs with specific accuracy for continuous inputs. Because of the lack of information about internal processes and boundary conditions in a heat transfer process, using neural networks is a proper method for modeling heat transfer problems [22–24].

As explained before, the cisterns are useful for storing thermal energy. Up to now, methods other than ANNs have been used to analyze thermal energy storage in cisterns. Artificial neural networks are data-driven methods, and so they can model the cistern without any information about boundary conditions or internal processes. Thus, in this Note, this method is used to model thermal energy storage in a cistern and to compare it with observational data.

Case Study

To use the neural networks for modeling heat transfer in cisterns, an underground cold-water storage reservoir was selected to evaluate its thermal performance. The cistern is located in one of the suburban areas of Yazd city, in which such an underground reservoir is used for serving cold drinking water to the residents. The storage system under investigation has a cylindrical underground storage reservoir that is 12 m in height and 12 m in diameter. It has four wind towers at its four corners, each about 10 m in height.

A tap used for cold-water discharge is located about 0.9 m above the reservoir bottom to prevent sediments created during past years from blocking the water's way out of the tap. This storage tank is responsible for serving around 1000 residents in the local community during six months from the end of April until mid-September, with an average daily water consumption of about 5.5 liters per person. Hence, the consumption pattern used in the present experimental work is based on the preceding assumptions. The storage reservoir is filled with 15°C water up to 10 m from the bottom of the tank in winter (January 2002) and left intact until the end of April, when the water discharge cycle is commenced. For measuring the temperature distribution in the vertical direction, 36 temperature sensors are placed inside the tank, each 0.3 m apart. The air temperature in the space around the outlet tap is also measured. Two 20-channel digital temperature displays are used to collect the data. Temperature data are collected every 10 days starting from 30 April 2002. Outside ambient temperature data is also obtained from the Yazd Weather Bureau. In Fig. 1, a schematic figure of a cistern is shown.

Architecture and Training Algorithm of the Artificial Neural Networks

Multilayer Feedforward Network Training by a Back-Propagation Algorithm

In this research, the multilayer feedforward network training by a back-propagation algorithm has been used. In this network, the number of input- and output-layer neurons is defined with the problem under study. For the current problem, ambient temperature data, the level of considered points from the bottom of the cistern, and the date are used to obtain the considered temperature at the specific level of the cistern on a specific date. The number of layers of the network and the number of neurons in these layers cannot be determined like the input and output layers. These parameters are determined using a trial-and-error process to obtain the best architecture of the network. The following equation describes network behavior:

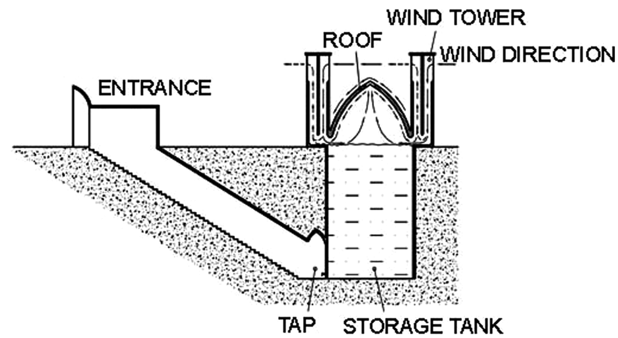

Fig. 1 A schematic view of the underground cold-water reservoir.

$$a^0 = P, \qquad a^{L+1} = f^{L+1}(\omega^{L+1} a^L + b^{L+1}), \qquad L = 0, 1, 2, \ldots, L-1 \tag{1}$$

In this equation, L is the number of network layers and P is the input vector of the network. On the other hand, P is the input of the first layer. The answer of the network is equal to a^L. The indicator of the optimized answer in the back-propagation algorithm (BP) is least-squares.

This network is a supervised network: that is, there should be an output for each input. The learning data pairs in the BP network can be as follows:

$$\{(P^1, T^1), (P^2, T^2), \ldots, (P^i, T^i)\} \tag{2}$$

where P^i is the input vector of the network and t^i is the target vector for input P^i. The error signal in the neuron of the output layer (layer L) in the Kth frequency, is obtained from the following equation:

$$e_j(k) = t_j(k) - a_j(k) \tag{3}$$

where $t_j(K)$ is the Jth element of the answer vector related with input vector $P(K)$. Only output neurons are observable neurons, and hence the behavior of the network is evaluated with the following equation:

$$F(k) = \sum_{j=1}^{S^L} e_j^2(k) \tag{4}$$

where S^L is the number of neurons in layer L.

The neural network model is calibrated by a training collection, which means that the parameters of the model, such as weights and biases, are calculated. One of the most important factors in network training is the number of epochs that the network performs during the training process. In the training process of a network, as the number of epochs increase, the difference between the target and answer of the network decreases. However, if there are excess epochs, the testing group's error increases too. The best number of training epochs is the value at which the errors in both the testing and training groups are minimized.

Data Preparation

Data must be prepared before the process. The main point in data preparation, before processing by neural network, is changing the data scales and locating them in domains. Whereas the change domain of the tangent-sigmoid activation function used in the hidden layer in all networks is between 1 and −1 and the slope of this function is considerable at around 1 and −1, in this research, for preventing network saturation, all data change scale and have been located between 1 and −1.

Calibration Parameters of Multilayer Feedforward Perceptron

Calibration parameters of neural networks include the number of hidden layers, transfer functions of each layer, number of neurons in each hidden layer, initial weights of the network, and learning rate. In this research, a multilayer feedforward perceptron (MLP) neural network is used, the transfer function that used in the hidden layer is tangent-sigmoid, and the transfer function of the output layer is linear. The number of neurons in the hidden layer is determined with a trial-and-error process. The initial weights of the network are determined by random numbers with unique distribution. Also, the behavior of variables and their correlation during the period may be changed; thus, a fixed learning rate may not be optimized. Therefore, the learning rate is considered to be variable with time, and for this purpose, the rate of performance function in each epoch is used, but the value of learning rate is limited to 10^{-2} and then the maximum performance function is defined. The maximum performance function (sum of the squared errors between the modeling and experimental values) is the highest acceptable limit of the performance function that should be satisfied in each sequence.

Modeling the Cistern by ANNs

In this research, various networks with various sizes and training functions have been used to obtain a temperature profile in a cistern. Inputs of the network are the ambient temperature on a specific date, the level of considered points from the bottom of the cistern, and the considered date that is specified for measuring the ambient temperature. The output of this network is the temperature at the specified levels from the bottom of the cistern at the date that is specified in the input. This network estimates one parameter from three parameters, and due to this estimation, the architecture of this network includes three neurons in the input layer and one neuron in the output layer. Because one parameter is estimated from three parameters, the error rate of the network is very low.

Among various training functions, the gradient-descent method and gradient-descent method with momentum have too many errors and, as shown in Figs. 2 and 3, their deviation from the ideal line is too high. In these figures, scatter plots of modeling values with respect to observation values have been shown.

The gradient-descent method with a variable learning rate presents a better answer than the two mentioned training functions (Fig. 4), but the gradient-descent method with a variable learning rate and momentum presents the best answer in comparison with the other 3 previous training functions (Fig. 5).

Eventually, the best training function that is suggested is the gradient-descent method with a variable learning rate and momentum. For choosing the best architecture, networks train with various numbers of neurons in the hidden layer, and the results

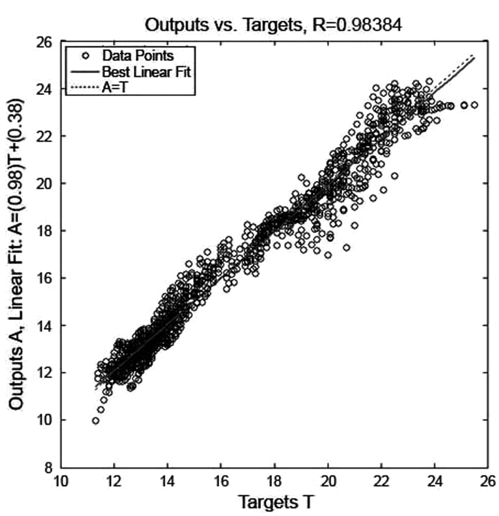

Fig. 2 Scatter plot for modeling values with respect to observational values; training function is gradient descent (20 neurons in the hidden layer).

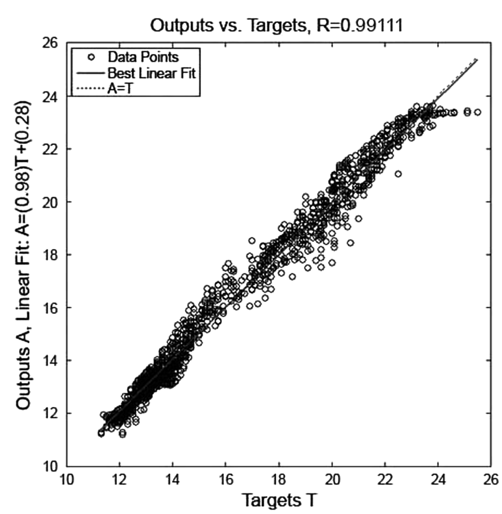

Fig. 4 Scatter plot for modeling values with respect to observational values; training function is gradient descent with variable learning rate (20 neurons in the hidden layer).

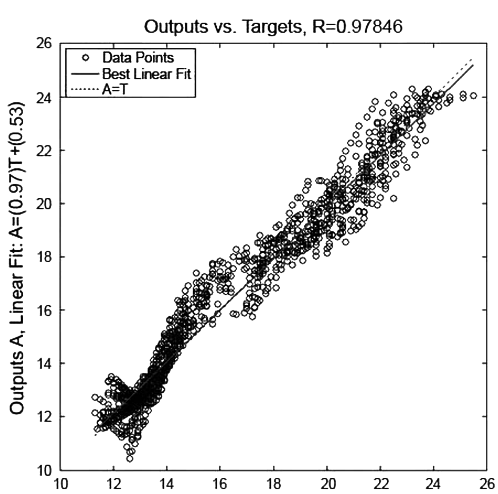

Fig. 3 Scatter plot for modeling values with respect to observational values; training function is gradient descent with momentum (20 neurons in the hidden layer).

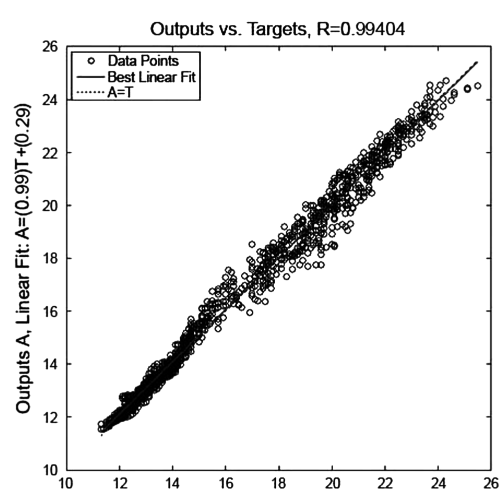

Fig. 5 Scatter plot for modeling values with respect to observational values; training function is gradient descent with variable learning rate and momentum (20 neurons in the hidden layer).

Table 1 Various architectures of the network that used the gradient-descent method with variable learning rate and momentum as training functions

Number of neurons in the hidden layer	3	5	10	15	20	25	30
Perf	1324.4	328.065	301.577	288.866	228.107	235.919	243.426
M	0.9248	0.9808	0.9829	0.9839	0.9867	0.9849	0.9860
B	1.2244	0.3164	0.2753	0.2552	0.2158	0.2448	0.2284
R	0.9616	0.9906	0.9914	0.9918	0.9935	0.9925	0.9928

obtained are shown in Table 1. In the first row of the table, various numbers of the hidden layer's neurons are shown. In the second row, performance functions of the network that is the sum of the squared error between the experimental data and the model are shown. As shown in the second row, performance functions do not decrease if the number of neurons in the hidden layer increases more than 20. In the third row, the slope of the regression line in the scatter plot is shown (the ideal number for the slope is 1). At the fourth row, the y intercept of the regression line in the scatter plot is shown (the ideal number for it is 0). At the fifth row, the correlation coefficient between the ANN's output and observations are shown (the ideal number for values of this row is 1).

Results

Figures 6–8 show the calculated temperature for June, August, and September, respectively, by an ANN. In this network, the calibration parameter of the number of hidden layers is 20, the training function is the gradient-descent method with a variable learning rate and momentum, and the back-propagation algorithm method has been used to determine weights and biases of this network. It is observed that the difference of obtained temperature profiles from both observation and the neural network is low; the neural network with mentioned specifications has an estimated temperature in the various heights and also in different time periods with infinitesimal error rate. It can be observed from the figures that the error rate is very low. In Fig. 9, the error plot and the difference of obtained temperature from both observation and the neural network on different days and at different levels of heights have been drawn. It can be seen in this figure that in most of the points the temperature difference is among the obtained values from the neural network and the observational measurement is less than 0.5°C.

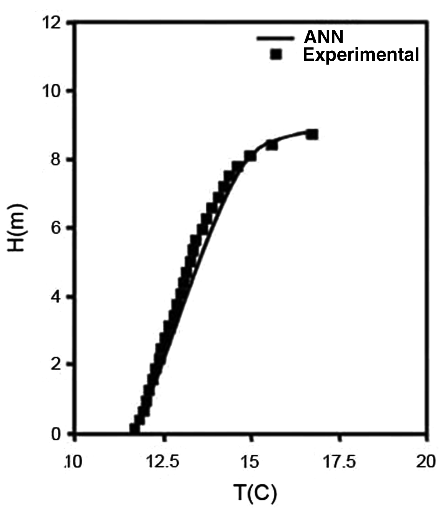

Fig. 6 Temperature changes in depth for observational and neural network results in the cistern during June.

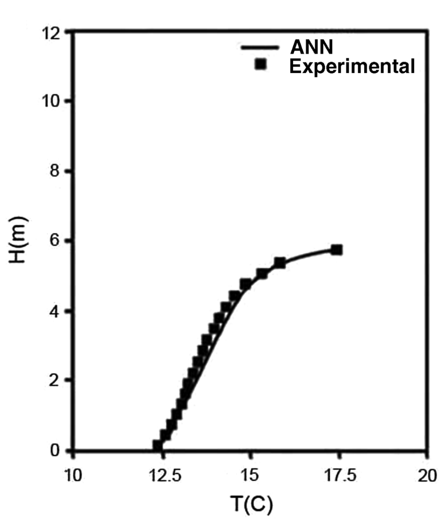

Fig. 7 Temperature changes in depth for observational and neural network results in the cistern during August.

Conclusions

Thermal layering of a long-term cold-water underground reservoir was studied using an ANN, and the results were compared with obtained thermal layering from observation data. For comparison performance of network modeling with various calibration methods, a multilayer feedforward perceptron (MLP) neural network with various architectures and training functions was performed. Various architectures of the network were calibrated and the results were compared with each other. It was found that the results from ANNs are in good agreement with observational data.

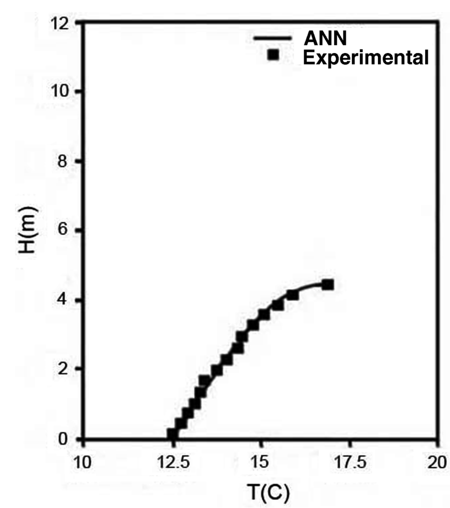

Fig. 8 Temperature changes in depth for observational and neural network results in the cistern during September.

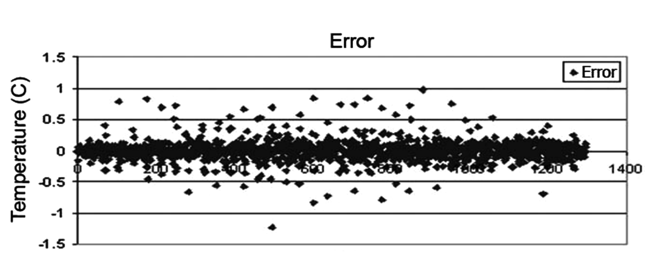

Fig. 9 Error plot and the difference between observational values and obtained values by MLP.

The thermal layering was stabilized in the cistern and kept stable during the discharge period. Because of thermal exchange among the upper layers of water and the dome, transfer of mass, and evaporative heat resulting from entry air from the wind towers, it was observed that the temperature distribution is linear in lower areas and it is exponential in upper areas.

It should be noted that thermal layering exists in thermal-energy-saving systems and in other reservoirs, such as cylindrical and noncylindrical solar storage tanks, underground saving tanks of cooling and warming energy, lakes, and solar ponds. Because of the fact that it is not possible to perform observational tasks in all situations and conditions, due to expensive expenditure for experimental research, the ANN method could be used for analysis of cisterns and existing underground cold water in other zones, which is much cheaper than experimental research.

References

[1] Dincer, I., and Rosen, M. A., *Thermal Energy Storage Systems and Applications*, Wiley, New York, 2002.

[2] Saito, A., "Recent Advances in Research on Cold Thermal Energy Storage," *International Journal of Refrigeration*, Vol. 25, No. 2, Mar. 2002, pp. 177–189.
doi:10.1016/S0140-7007(01)00078-0

[3] Nelson, J. E. B., Balakrishnan, A. R., and Murthy, S. S., "Parametric Studies on Thermally Stratified Chilled Water Storage Systems," *Applied Thermal Engineering*, Vol. 19, No. 1, Jan. 1999, pp. 89–115.
doi:10.1016/S1359-4311(98)00014-3

[4] Nelson, J. E. B., Balakrishnan, A. R., and Murthy, S. S., "Experiments on Stratified Chilled-Water Tanks," *International Journal of Refrigeration*, Vol. 22, No. 3, May 1999, pp. 216–234.
doi:10.1016/S0140-7007(98)00055-3

[5] Al-Marafie, A. M. R., "Stratification Behavior in Chilled Water Storage Tank," *International Journal of Refrigeration*, Vol. 10, No. 6, Nov. 1987, pp. 364–366.
doi:10.1016/0140-7007(87)90125-3

[6] Suri, R. K., Al-Marafie, A. M. R., Maheshwari, G. P., Al-Juwayhel, F., Al-Jandal, S., Al-Madani, K., and Aburshid, H., "Experimental Investigation of Chilled Water Storage Technique for Peak Power Shaving," *International Journal of Refrigeration*, Vol. 12, No. 4, July 1989, pp. 213–219.
doi:10.1016/0140-7007(89)90046-7

[7] Alizadeh, S., "An Experimental and Numerical Study of Thermal Stratification in a Horizontal Cylindrical Solar Storage Tank," *Solar Energy*, Vol. 66, No. 6, Sept. 1999, pp. 409–421.
doi:10.1016/S0038-092X(99)00036-5

[8] Gursu, S., Sherif, S. A., Veziroglut, T. N., and Sheffield, J. W., "Analysis And Optimization Of Thermal Stratification and Self-Pressurization Effects in Liquid Hydrogen Storage Systems, 1: Model Development," *Journal of Energy Resources Technology*, Vol. 115, No. 3, 1993, pp. 221–227.
doi:10.1115/1.2905997

[9] Pietrzyk, J. R., and Hepworth, H. K., "Analysis of Thermal Stratification in Cryogen Storage Tanks Under Quiescent, Microgravity Conditions," 27th AIAA, SAE, ASME, and ASEE, Joint Propulsion Conference, AIAA Paper 1991-2327, June 1991.

[10] Altuntop, N., Arslan, M., Ozceyhan, V., and Kanoglu, M., "Effect of Obstacles on Thermal Stratification in Hot Water Storage Tanks," *Applied Thermal Engineering*, Vol. 25, Nos. 14–15, Oct. 2005, pp. 2285–2298.
doi:10.1016/j.applthermaleng.2004.12.013

[11] Li, Z. F., and Sumathy, K., "Performance Study of a Partitioned Thermally Stratified Storage Tank in a Solar Powered Absorption Air Conditioning System," *Applied Thermal Engineering*, Vol. 22, No. 11, Aug. 2002, pp. 1207–1216.
doi:10.1016/S1359-4311(02)00048-0

[12] Kerkeni, C., BenJemaa, F., Kooli, S., Farhat, A., and Belghith, A., "Solar Domestic Hot Water: Numerical and Experimental Study of the Thermal Stratification in a Storage Tank," *2000 Mediterranean Conference for Environment and Solar*, Inst. of Electrical and Electronics Engineers, Piscataway, NJ, 2000, pp. 195–199.
doi:10.1109/CMPLES.2000.939897

[13] Bahadori, M. N., and Haghighat, F., "Long-Term Storage of Chilled Water in Cisterns in Hot, Arid Regions," *Building and Environment*, Vol. 23, No. 1, 1988, pp. 29–37.
doi:10.1016/0360-1323(88)90015-7

[14] Dehghan, A., "An Experimental Investigation of Thermal Stratification in an Underground Water Reservoir," *2004 ASME Heat Transfer/Fluids Engineering Summer Conference*, American Society of Mechanical Engineers, New York, July 2004, pp. 1–4.

[15] Olmsted, D. D., "History and Principles of Neural Networks to 1960," http://www.neurocomputing.org/NNHistoryTo1960.aspx.

[16] McCulloch, W., and Pitts, W., "A Logical Calculus of the Ideas Immanent in Nervous Activity," *Bulletin of Mathematical Biophysics*, Vol. 5, 1943, pp. 115–133.
doi:10.1007/BF02459570

[17] Weinbaum, S., "A Hypothesis for Vulnerable Plaque Rupture Due to Stress-Induced Debonding Around Cellular Micro Calcifications in Thin Fibrous Caps," *Proceedings of the National Academy of Sciences of the United States of America*, National Academy of Sciences, Washington, D.C., Mar. 2007, pp. 5–6.
doi:10.1073/pnas.0606310103

[18] Islamoglu, Y., "Experimental and Numerical Analysis of Heat Transfer in Corrugated Duct," Ph.D. Thesis, Sakarya Univ., Adapazari, Turkey, 2002.

[19] Islamoglu, Y., Halici, F., and Parmaksizoglu, C., "A Computer Aided Analysis of Heat Transfer in Plate Heat Exchanger Channels with Experimental Confirmation," *Proceedings of the Russian National Symposium on Power Engineering*, 2001, pp. 256–261.

[20] Diaz, G., Sen, M., Yang, K. T., and McClain, R. L., "Dynamic Prediction and Control of Heat Exchangers Using Artificial Neural Networks," *International Journal of Heat and Mass Transfer*, Vol. 44, No. 9, May 2001, pp. 1671–1679.
doi:10.1016/S0017-9310(00)00228-3

[21] Pacheco-Vega, A., Diaz, G., Sen, M., Yang, K. T., and McClain, R. L., "Heat Rate Predictions Air–Water Heat Exchangers Using Correlations and Neural Networks," *Journal of Heat Transfer*, Vol. 123, No. 2, 2001, pp. 348–354.
doi:10.1115/1.1351167

[22] Sablani, S. S., Kacimov, A., Perret, J., Mujumdar, A. S., and Campo, A., "Non-Iterative Estimation of Heat Transfer Coefficients Using Artificial Neural Network Models," *International Journal of Heat and Mass Transfer*, Vol. 48, Nos. 3–4, Jan.–Feb. 2005, pp. 665–679.
doi:10.1016/j.ijheatmasstransfer.2004.09.005

[23] Islamoglu, Y., and Kurt, A., "Heat Transfer Analysis Using ANNs with Experimental Data for Air Flowing in Corrugated Channels," *International Journal of Heat and Mass Transfer*, Vol. 47, Nos. 6–7, Mar. 2004, pp. 1361–1365.
doi:10.1016/j.ijheatmasstransfer.2003.07.031

[24] Tsang, T. H., Edgar, T. F., and Hougen, J. O., "Estimation of Heat Transfer Parameters in a Packed Bed," *Chemical Engineering Journal (Lausanne)*, Vol. 11, No. 1, 1976, pp. 57–66.
doi:10.1016/0300-9467(76)80006-8